

Research paper

Model-free based adaptive nonsingular fast terminal sliding mode control with time-delay estimation for a 12 DOF multi-functional lower limb exoskeleton



Shuaishuai Han, Haoping Wang*, Yang Tian

School of Automation, LaFCAS, Nanjing University of Science & Technology, Nanjing 210094, China

ARTICLE INFO

Keywords:
 12 DOF lower limb exoskeleton
 Model free control
 Time-delay estimation
 Adaptive terminal sliding mode

ABSTRACT

The design of a 12 DOF lower limb multi-functional exoskeleton is realized in SolidWorks with the analysis of kinematics. For controller design, this paper presents the model-free based adaptive nonsingular fast terminal sliding mode control which comprises three parts: the intelligent PI controller, time-delay estimation, and adaptive sliding mode compensator. The proposed control strategy drives tracking errors to a nonsingular fast terminal sliding surface and realizes fast convergence in finite time. The designed adaptive law approximates the upper bound of estimation error in time-delay estimation and thus it reduces the fundamental chattering on the switching manifold. The stability of controller is verified by using Lyapunov theory. To validate the proposed method, the virtual prototype is transferred to MATLAB/SimMechanics as a platform for co-simulation. The proposed method shows improved tracking performance compared with the existing model free controller in co-simulations.

1. Introduction

Since 1960s, exoskeletons have been developed prosperously, in different types of mechanical structures, actuators and interfaces. Lower limb power assistance or rehabilitation exoskeletons have been a hot research area for decades and plenty of them have been successfully applied until now. With the overview of currently available lower limb exoskeletons, Lokomat [1], ALEX [2] and Ekso [3] are mainly applied for gait rehabilitation during the therapy for gait disorder caused by stroke, spinal cord injury, brain injury, etc. Those rehabilitation devices usually cooperate with treadmills [1,2] or canes [3] for balance and security during gait training. For human locomotion assistance, Ekso [3], ReWalk [4], CUHK-EXO [5], and Vanderbilt exoskeleton [6] all have to be equipped with canes as guide and support. Their focus is concentrated on regaining walking abilities for the lower limb disabled. BLEEX [7], HAL [8] and HEXAR [9] try to augment human strength for load carrying (in soldier's tasks or worker's heavy support work). Those exoskeletons above have been efficiently implemented and made contributions to various groups. However, most of the existing devices focus on some specific operations because of the complexity of human-robot system, limitation of mechanical design and materials, difficulties in controller design and intention recognition, and etc [10]. There is still great room for improvement.

To cover all the situations above and broaden possible applications, the authors give a multi-functional and modular design of a 12 DOF lower limb exoskeleton. Multi-DOF equipment guarantees the accomplishment of different movements. With adjustable length of links, the exoskeleton can fit various users with different body size. Modular design can realize single joint rehabilitation or power assistance instead of wearing entirely the relatively heavy device. In rehabilitation area, gait training and correction is still the main field with broad research and experimental applications [10]. Compared to conventional biped robots whose walking tasks usually focus on the balance strategy and path planning, a lower limb exoskeleton usually deals with much more complex conditions. For current control research, this paper will mainly focus on an online adjustable rehabilitation task.

Various strategies have been provided and get continuously developed for the control of robotic dynamic systems. The complexity of physical plant with unknown uncertainties and dynamics variations, has hindered the development of classic inverse dynamics method [11,12] which is usually combined with other techniques, such as sliding mode control (SMC), adaptive control, fuzzy control [12], neural networks(NNs) [11], etc. For nonlinear time-varying and uncertain systems, NNs have excellent approximation ability and fuzzy control possesses remarkable robustness and adaptivity. However, numerous parameters tuning and complex rules may decrease the

* Corresponding author.

E-mail address: hp.wang@njust.edu.cn (H. Wang).

efficiency and possibility of them.

Sliding mode control (SMC) has attractive advantages of robustness to uncertainties and disturbances and low sensitivity to the system parameter variations. Terminal SMC (TSMC) [13] is particularly useful for high precision control as it speeds up the rate of convergence near the equilibrium point and the states will reach the desire ones in finite time. In [14], a nonsingular TSMC (NTSMC) was proposed to avoid the singularity in conventional TSMC, which may be lead to during the reaching phase. A novel nonsingular fast TSM control (NFTSMC) structure proposed in [15] realized fast convergence without any singularity occurrence in finite time.

Adaptive SMC (ASMC) [16–19] was proposed for the elimination of fundamental chattering in SMC by adaptive gain tuning. Literature [16] tried to solve the fundamental chattering problem according to a linear sliding surface and adaptive gain tuning law based on Lyapunov function design, but can only achieve bounded stability instead of asymptotic stability. Although [17] avoided the singularity occurrence and achieved faster convergence, the controller can only achieve bounded stability instead of asymptotic stability in finite time.

Some advanced strategies for model independence realization have received increasing attention such as active disturbance rejection control (ADRC) [20], date-driven control (DDC) [21,22], time-delay control (TDC) [23], repetitive learning control (RLC) [24], model free control (MFC) [25–27], etc., whose controllers design mainly rely on the input-output (I/O) data. Developed by Han in [20], ADRC technique depends on extended state observer (ESO) whose convergence speed will have crucial impact on control quality. Based on the data model idea, DDC can be combined with optimization [22] or adaptive control [21] to form a data-based control structure. TDC [16,17] was proposed with time delay estimation (TDE) which is an online system dynamics estimation method. A kind of algebraic identification based MFC was proposed by Fliess and Join [25] and has been applied to some simple or slow time-varying physical systems. An attractive “ultra-local model” idea was introduced for order reducing in [25].

Up to now, few literatures involve the application of TDC or MFC method to lower limb exoskeleton systems. Our research tries to propose a model independent strategy on the basis of “ultra-local model” which is an efficient order reduction method and then present the corresponding intelligent PI (iPI) controller. For uncertainties measurement and avoiding complex algebraic calculation as [25], time-delay estimation (TDE) technique which is easy-to-use and possesses robustness to uncertainties is employed to estimation the *lumped total disturbance*, forming the model free structure TDE-iPI.

For the elimination of TDE deduced errors, Wang et al. [27] adopted NTSMC as a control input compensator and combined it to TDE-iPD controller. However, the upper bound of estimation error was assumed to be a known value which is not always possible in practical applications. The upper bound, i.e., the switching gain in controllers is usually chosen to be large enough to cover the possible error values and guarantee the stability. In such a case, chattering will be increased. With suitable estimation technique, the unknown upper bound may be approximated so as to reduce the chattering without instability. An adaptive law is designed in this paper and the convergence is guaranteed by Lyapunov stability analysis. Because of the adaptive switching gain tuning, the chattering gets reduced during the sliding period. To achieve fast tracking and finite time convergence, NFTSMC is used to deal with the state space equations resulting from TDE-iPI controller. Thus, developed from [27], a model-free based adaptive NFTSMC (MFANFTSMC) is finally proposed for the designed 12 DOF lower limb exoskeleton. This is also a further research of our previous work in [28].

The characteristics of proposed control structure can be summarized as: (1) the process of parameter tuning is much simplified and can be determined by conventional frequency-domain analysis theory; (2) few experiments will be conducted on the real physical system during the controller design and such advantage will reduce the difficulty of dynamic analysis in exoskeleton controlling; (3) with the sliding surface

design and adaptive switching gain, the fast convergence in finite time and chattering reduction can be realized.

The rest of this paper is organized as follows. In Section 2, the mechanical design of 12 DOF multi-functional modular lower limb exoskeleton is realized in SolidWorks. Section 3 deals with the analysis of forward and inverse kinematics. The novel MFANFTSMC method and stability analysis are given in Section 4. Section 5 gives the simulation results to compare the MFC with MFANFTSMC and illustrates the improvement of the proposed controller. Finally, Section 6 is dedicated for the conclusion and future work.

2. Mechanical design and virtual prototype realization

The multi-functional and modular exoskeleton design is conducted for the application of rehabilitation or power assistance. To meet the walking requirements and improve the comfortableness of human operator, the design includes DOF configuration and dimension determination. Then the virtual prototype is designed and realized with Solidworks.

2.1. 12 DOF configuration

The human leg can be thought of as a 7 DOF structure in general, with three rotational DOFs at the hip, one at the knee and three at the ankle. Lots of complex movements can be accomplished thanks to its multi-DOF biological structure while physical machine can hardly do. Thus, suitable DOF assignment of lower limb exoskeleton can fulfill basic movements and realize various operations. According to human biological characteristics [29,30], the corresponding approximate moving limitation can be summarized as Table 1, where E/F, A/A, E/I is the abbreviations of extension/flexion, abduction/adduction and extorsion/intorsion, respectively.

Accordingly, the DOF assignment and virtual prototype can be shown in Fig. 1.

The details of virtual prototype will be given in Section 2.2. Apparently, the increase of DOFs will enhance the difficulty of exoskeleton controlling. In the precondition of satisfying the moving requirements, the DOFs are set to be 12, i.e., there are 6 DOFs per leg. In practical walking conditions (straight walking especially), extorsion/intorsion DOF in ankle is almost not in use, and it can be ignored in the exoskeleton design to reduce control difficulty. Besides, to improve the comfort level of human operators, the abduction/adduction DOF in ankle is designed as a passive one (without actuator).

2.2. Virtual prototype realization

To establish a suitable virtual prototype of the lower limb exoskeleton for further research, the human body size should be considered. The dimension of our exoskeleton refers to the size of human body and is determined to fit the average size. To prevent the possible discomfort and injuries, the length of each link is changeable and the attachments which are fixed to human legs can rotate according to walking movements. Fig. 2(a) gives a further view of this exoskeleton.

Table 1
The DOF distribution and motion range (°).

Joint DOF	Limitation	Walking range
Hip E/F	–10–140	–10–40
Hip A/A	–20–45	–3–5
Hip E/I	–70–90	–3–7
Knee E/F	0–135	0–67
Ankle E/F	–60–27	–20–20
Ankle A/A	<10	≈0
Ankle E/I	–30–30	≈0

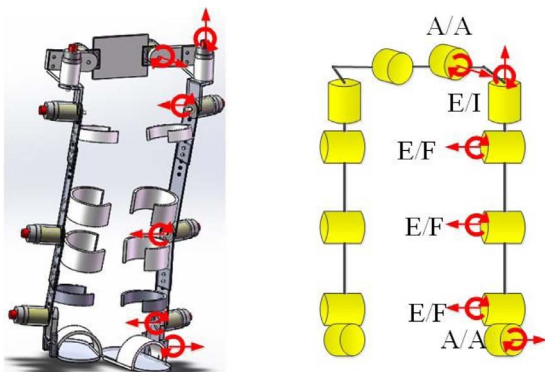


Fig. 1. The DOF assignment and virtual prototype of exoskeleton.

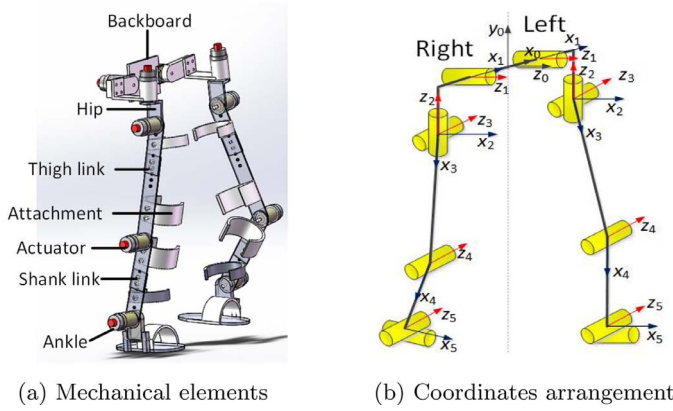


Fig. 2. Mechanical structure of exoskeleton.

The hip contains three degrees of freedom to expand the capabilities of walking, direction tuning, sit-stand and other daily movements.

Based on the mechanical configuration above, the entire hardware platform can be divided into several modular parts for multi-function realization, which are depicted in Fig. 3.

The hip exoskeleton is equipped with 3 DOFs in Fig. 3(a), i.e., hip E/F, A/A and E/I for hip rehabilitation or power assistant without any constraints. (b) extends the assistant ability to the knee joint. (c) is a fully articulated lower limb exoskeleton for various tasks like gait assistance of paraplegic patient [1], sit to stand transfer and stair climbing of the aged and disabled, power assistance of soldiers or workers. Cooperating with a treadmill and body weight support in Fig. 3(d), the entire exoskeleton platform forms a stationary gait rehabilitation system for the patients with gait disorders or other lower limb injuries.

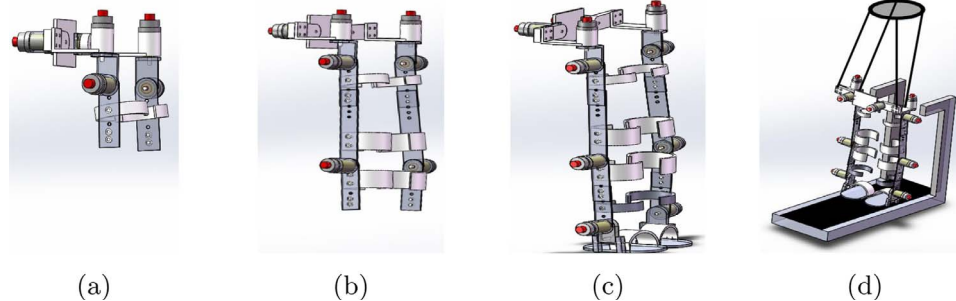


Fig. 3. Modular design of the exoskeleton.

Table 2
The D-H parameters.

Right					Left				
Link	θ_{ri}	$a_{r(i-1)}$	d_{ri}		Link	θ_{li}	$a_{l(i-1)}$	d_{li}	
1	θ_{r1}	0	-0.31	0	1	θ_{l1}	0	-0.13	0
2	θ_{r2}	$-\pi/2$	-0.045	-0.139	2	θ_{l2}	$-\pi/2$	0.045	-0.139
3	θ_{r3}	$-\pi/2$	0	0	3	θ_{l3}	$-\pi/2$	0	0
4	θ_{r4}	0	0.465	0	4	θ_{l4}	0	0.465	0
5	θ_{r5}	0	0.37	0	5	θ_{l5}	0	0.37	0

3. Kinematic analysis

To establish the connection between two links, D-H principle is widely used which is given by Denavit and Hartenberg [31]. The modified D-H method was proposed in [32] and reduced the complexity of kinematic calculation. By the modified D-H method, the relation between the end-effector and base coordinate can be established. For each link, a Cartesian coordinate system will be defined to describe the pose and usually z -axis is the rotation axis. The relation of different coordinate is transformed by a 4×4 matrix which contains four parameters.

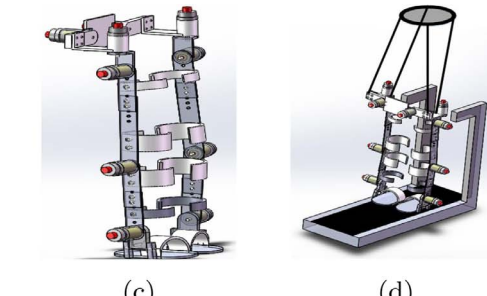
Because of the symmetrical structure, it is convenient to choose the center of the two hip joints as the base coordinate, which is denoted as $x_0y_0z_0$. The detailed coordinates arrangement is showed in Fig. 2(b), where the y -axis can be determined by right-hand rule and is ignored here for simplicity.

The passive DOF in ankle is ignored here and the extension/flexion DOF in each ankle is set to be the end-effector of each limb. The D-H parameters based on the analysis in Section 2.2 are summarized as Table 2 where r, l denote the right leg and left leg, respectively. In consideration of the symmetrical structure, the kinematics are same for each single leg, so the subscript r, l are omitted in the following content.

In practical applications, especially the rehabilitation tasks, the trajectory tracking of the end-effector is usually the control target. However, for the controller (actuator), the desired joint angle should be the desired input. In such a case, the so called inverse kinematics are needed, which give the desired angle of each joint according to the desired trajectory represented by p_x, p_y, p_z . This paper is devoted to deal with the gait rehabilitation in the straight walking conditions during which the hip extension/flexion and abduction/adduction DOFs almost stay in a constant joint angle. In such cases, to get the solution of inverse kinematics, two constraints are given as follow:

- (i) $\theta_3 + \theta_4 + \theta_5 = 0$: the palm of foot is parallel to the ground;
- (ii) θ_2 is a constant: to simplify the condition of direction changing in walking tasks.

According to the constraints above, the solution of inverse kinematics [33] can be obtained as Eq. (1)



$$\begin{cases} \theta_1 = -a \tan 2 \left(\frac{a_2 s_2 - p_z c_2}{s_2}, \pm \sqrt{(p_x - a_1)^2 + p_y^2 - \left(\frac{a_2 s_2 - p_z c_2}{s_2} \right)^2} \right) + a \tan 2(p_x - a_1, p_y) \\ \theta_2 = -\pi/2 \theta_3 = -a \tan 2(m, \pm \sqrt{(a_4 + a_5 c_4)^2 + a_5^2 s_4^2 - m^2}) + a \tan 2(-a_5 s_4, a_4 + a_5 c_4) \\ \theta_4 = \arccos \left(\frac{(p_x c_1 + p_y s_1 - a_1 c_1 - a_2) c_2 - s_2 p_z - a_3)^2 + m^2 - a_4^2 - a_5^2}{2 a_4 a_5} \right) \\ \theta_5 = -\theta_3 - \theta_4 \end{cases} \quad (1)$$

with $m = -p_x s_1 + p_y c_1 + a_1 s_1 - d_2$, where $\theta_2 = -\pi/2$ denotes the straight walking condition, s_i, c_i represent $\sin \theta_i, \cos \theta_i$ respectively, p_x, p_y, p_z are the position of end effector with regard to the base coordinate, which also can be defined as the foot position (represented by the ankle joint here) for the further control task. In the inverse kinematics solution, the main parameters are all represented by corresponding letters so that it will hold for both limbs.

4. Controller design

This research focuses on walking rehabilitation. To satisfy different training requirements, the training trajectories can switch between different modes, faster or slower, forming the online adjustment. Our proposed MFANFTSMC with the combination of TDE-iPI sub-controller and ANFTSMC sub-controller is depicted as Fig. 4.

In TDE-iPI sub-controller, an *ultra-local model* is defined for dynamics restructuring and the lumped unknown dynamics \hat{F} is obtained by TDE. Intelligent PI controller is thus designed. ANFTSMC tries to eliminate the error caused by TDE. Adaptive law in ANFTSMC sub-controller aims at reducing chattering without losing the robustness to error or uncertainties. Fig. 4 presents the control structure of an online gait adjustable rehabilitation mode, where the desire gait q_d is generated from two parts: basic off-line trajectory planning part q_r and human intention part q_h . At the beginning, human legs will be entirely in a passive state without any moving intention and the operator may adjust the training gait to a lower or higher level at any moment. When q_h occurs, the training gait q_d will switch to another mode after a transient period. The designed controllers need to be adaptive to the gait switch and guarantee the stability. In joint-level, an independent controller should be designed for each joint to provide the actuation input according to its desired trajectory.

4.1. Time-delay estimation based intelligent PI control

4.1.1. Intelligent PI controller

Classic PID controller entirely ignores the analysis of model and

arises the problem of complex or even strange parameters tuning. In our proposed TDE-iPI structure, an “*ultra-local model*” idea which is also explained in detail in our previous work [34], is adopted for order reduction.

Generally, the dynamic model of a single limb can be formulated by Lagrangian dynamic equation [33]:

$$\tau_i = M(q_i)\ddot{q}_i + C(q_i, \dot{q}_i)\dot{q}_i + G(q_i) \quad (2)$$

where $i = l, r$ denotes left or right leg, $q_i = [\theta_{i1} \ \theta_{i2} \ \dots \ \theta_{i5}]^T$ indicates the angles of each joint. τ_i represents the torque vector exerting on joints. $M(q_i), C(q_i, \dot{q}_i), G(q_i)$ are the inertia matrix, Coriolis forces, gravitational forces, respectively. \dot{q}_i, \ddot{q}_i are joint velocities and accelerations. Considering the mapping between the joint angle, velocity and acceleration, the dynamics of a single limb can be formulated as:

$$\tau = H(q, \dot{q}, \ddot{q}) \quad (3)$$

where $H(q, \dot{q}, \ddot{q})$ is a 5×1 vector containing the complex information of mass-inertia, Coriolis, gravity and various possible uncertainties. For the convenience of illustration, $i = l, r$ is omitted.

To decrease the complexity of dynamic expression without losing the efficiency, the *ultra-local* order reduction principle in a sliding window is adopted to deal with the exoskeleton control and for the i th joint, the first order reduction modeling is depicted in Fig. 5.

$q^{(o)}(t)$ denotes o th order derivative of $q(t)$. At each sampling period (i.e. T_e) of calculator, i.e., a sliding window which is updated with time, each joint is a SISO (single-input single-output) plant and can be represented in the same form. Then the entire exoskeleton dynamics can be further formulated in a first order form:

$$\dot{q}(t) = q^{(1)}(t) = F(t) + \Lambda \tau(t) \quad (4)$$

where $\Lambda = \text{diag}\{\alpha_1, \alpha_2, \dots, \alpha_5\}$ is a diagonal and positive definite matrix which is a non-physical constant parameter and chosen by the practitioner such that $\Lambda \tau(t)$ and $\dot{q}(t)$ is the same magnitude. $F(t)$ which is called *lumped total disturbance* and continuously updated, is relative to time, effects of unmodeled dynamics and various disturbances. Such an ultra-local order reduction model builds an simple map relation

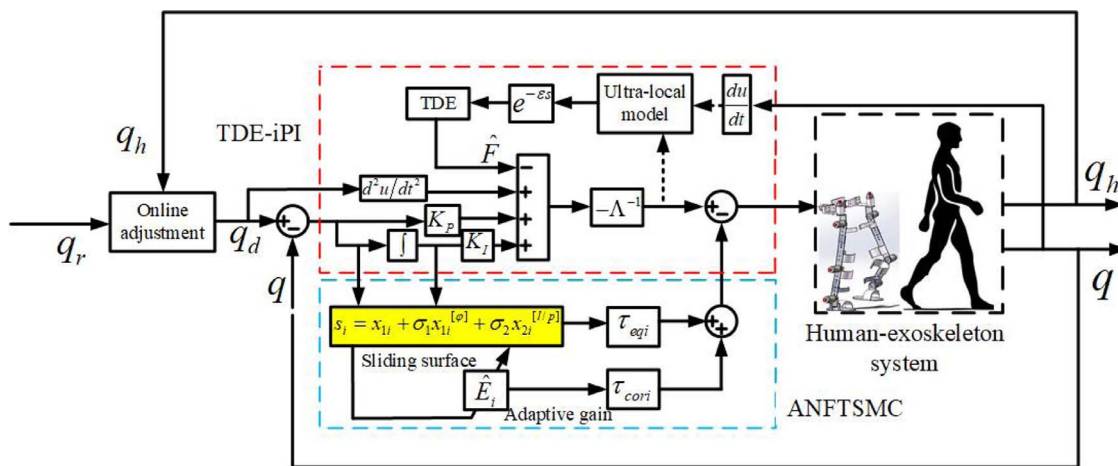


Fig. 4. Block diagram of the MAFNFTSMC.

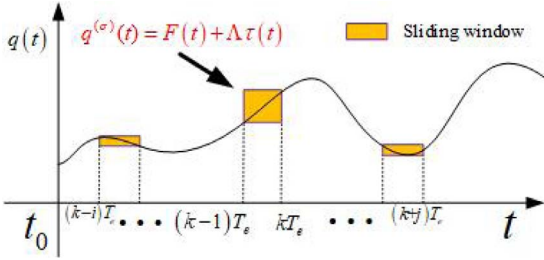


Fig. 5. Ultra-local order reduction modeling principle in a sliding window.

between $q(t)$ and $\tau(t)$.

The iPI controller [25,34] is designed as

$$\tau(t) = \Lambda^{-1} \left(\dot{q}_d(t) - F(t) + K_P e(t) + K_I \int_0^t e(\sigma) d\sigma \right) \quad (5)$$

where $q_d = [\theta_1^d \ \theta_2^d \ \dots \ \theta_5^d]^T$ denotes reference position and \dot{q}_d is the corresponding velocity. Error vector is $e = q_d - q = [\theta_1^d - \theta_1 \ \dots \ \theta_5^d - \theta_5]^T$. $K_P = \text{diag}\{K_{P1}, K_{P2}, \dots, K_{P5}\}$ and $K_I = \text{diag}\{K_{I1}, K_{I2}, \dots, K_{I5}\}$ are diagonal and positive definite gain matrices. Substituting Eq. (4) into Eq. (3) yeilds the error dynamics:

$$\dot{e}(t) + K_P e(t) + K_I \int_0^t e(\sigma) d\sigma = 0 \quad (6)$$

with $\dot{e} = \dot{q}_d - \dot{q}$. $F(t)$ in Eq. (4) is assumed to be known exactly and a linear differential equation with constant coefficients is deduced. The tuning of K_P, K_I becomes, therefore, straight forward for obtaining a good tracking of desire input. The process of parameter tuning can be determined by conventional frequency-domain analysis theory.

4.1.2. Time-delay estimation technique

Apparently, the estimation of $F(t)$ is a crucial issue for model free controller application. Different from the complex algebraic parameter identification technique [25], TDE technique [15,17,23] is applied to estimate $F(t)$. Under the assumption that the time delay ϵ is sufficiently small, following approximation is valid due to (3):

$$F(t) \approx \hat{F}(t) = F(t - \epsilon) = \dot{q}(t - \epsilon) - \Lambda\tau(t - \epsilon) \quad (7)$$

The time delay is used on purpose to apply the TDE technique to estimate and cancel nonlinear and uncertain terms of the exoskeleton dynamics. $F(t)$ is assumed to be continuous with respect to time. Therefore, $F(t - \epsilon)$ can be used to estimate $F(t)$ if the delay interval ϵ is small enough. Replacing the $F(t)$ by $\hat{F}(t)$, Eq. (5) becomes

$$\dot{e}(t) + K_P e(t) + K_I \int_0^t e(\sigma) d\sigma = e_{\text{est}} \quad (8)$$

where the TDE estimation error vector is denoted as $e_{\text{est}} = \hat{F}(t) - F(t) = [e_{\text{est}1} \ e_{\text{est}2} \ \dots \ e_{\text{est}5}]^T$.

4.2. Model-free based adaptive nonsingular fast terminal sliding mode control

4.2.1. Adaptive sliding mode compensator

To eliminate the estimation error e_{est} in Eq. (7), an additional sliding mode control [27] is designed further and it yields the following model-free based adaptive nonsingular fast terminal sliding mode control (MFANFTSMC)

$$\tau(t) = \Lambda^{-1} \times \left(\dot{q}_d(t) - \hat{F}(t) + K_P e(t) + K_I \int_0^t e(\sigma) d\sigma \right) - \tau_{sm} \quad (9)$$

where $\tau_{sm} = [\tau_{sm1} \ \tau_{sm2} \ \dots \ \tau_{sm5}]^T$ is an augmented adaptive sliding mode compensator which will be designed later. Then the closed loop equation can be updated as

$$\dot{e}(t) + K_P e(t) + K_I \int_0^t e(\sigma) d\sigma = e_{\text{est}} + \Lambda\tau_{sm} \quad (10)$$

Define the state variables:

$$x_1(t) = \int_0^t e(\sigma) d\sigma, x_2(t) = e(t) \quad (11)$$

The corresponding state-space equations are

$$\begin{cases} \dot{x}_1(t) = x_2(t) \\ \dot{x}_2(t) = -K_P x_2(t) - K_I x_1(t) + e_{\text{est}} + \Lambda\tau_{sm} \end{cases} \quad (12)$$

As the system is BIBS (Bounded Input Bounded State) and the derivative of its input is bounded, the estimation error is also assumed to be bounded, i.e., $|e_{\text{est}i}| \leq E_i, i = 1, 2, \dots, 5$. $E_i \geq \sup |e_{\text{est}i}|$ is a positive constant. A nonsingular fast terminal sliding surface (NFTSS) [15] is designed as:

$$s_i = x_{1i} + \sigma_1 x_{1i}^{|\varphi|} + \sigma_2 x_{2i}^{l/p} \quad (13)$$

where s_i is the sliding variable for the i th joint controller, σ_1, σ_2 are positive definite constants, l, p are positive odd numbers satisfying the relation $1 < l/p < 2$ and $\varphi > l/p$.

Notations: $x^{[c]} = |x|^c \text{sgn}(x)$, with $c > 0$.

It can be easily verified that as $c \geq 1$, $\frac{d}{dt}x^{[c]} = c|x|^{c-1}\dot{x}$. To ensure the sliding motion occurs, the following inequality should be satisfied:

$$\dot{s} < 0 \quad (14)$$

and the derivative of sliding surface is

$$\begin{aligned} \dot{s}_i &= x_{2i} + \sigma_1 \varphi x_{2i} |x_{1i}|^{|\varphi|-1} + \sigma_2 (l/p) \varphi |x_{2i}|^{l/p-1} \dot{x}_{2i} \\ &= x_{2i} + \sigma_1 \varphi x_{2i} |x_{1i}|^{|\varphi|-1} + \sigma_2 \frac{l}{p} \varphi |x_{2i}|^{l/p-1} (-K_P x_{2i} - K_I x_{1i} + \alpha_i \tau_{smi} + e_{\text{est}i}) \end{aligned} \quad (15)$$

To ensure the required condition (14), the augmented sliding mode control part is designed as:

$$\tau_{smi} = \tau_{eqi} + \tau_{cori} \quad (16)$$

$$\tau_{eqi} = (1/\alpha_i)(K_{Pi}x_{2i} + K_{Ii}x_{1i}) - \frac{p}{\alpha_i \sigma_2 l} x_{2i}^{[2-l/p]} (1 + \sigma_1 \varphi |x_{1i}|^{|\varphi|-1}) \quad (17)$$

$$\tau_{cori} = -(1/\alpha_i)(E_i + \lambda) \text{sgn}(s_i) \quad (18)$$

where τ_{eqi}, τ_{cori} are called *equivalent control law* and *correction control law*, respectively. λ is a positive constant. τ_{eqi} is obtained under the condition $\dot{s}_i = 0$. The role of the second term τ_{cori} is to force the system trajectories to reach the sliding surface, which will be deduced by Lyapunov stability analysis.

However, in practical operations, the upper bound E_i is unknown and usually chosen to be large enough to cover a wide range of uncertainties. Such large switch gain will cause much oscillation around the sliding manifold and large actuation torques. To approximate the upper bound of TDE error by \hat{E}_i , the adaptive law is designed

$$\dot{\hat{E}}_i = s_i \sigma_2 (l/p) \varphi |x_{2i}|^{l/p-1} \text{sgn}(s_i) \quad (19)$$

and E_i in τ_{smi} will be replaced by the estimation value \hat{E}_i .

Then the proposed MFNFTSMC controller can be obtained in joint- i :

$$\begin{aligned} \tau_i(t) &= (1/\alpha_i) \left(\dot{\hat{E}}_i^d - \hat{E}_i + K_{Pi} e_i + K_{Ii} \int_0^t e_i(\sigma) d\sigma \right) - (1/\alpha_i)(K_{Pi}x_{2i} + K_{Ii}x_{1i}) \\ &\quad + (1/\alpha_i)(\hat{E}_i + \lambda) \text{sgn}(s_i) + \frac{p}{\alpha_i \sigma_2 l} x_{2i}^{[2-l/p]} (1 + \sigma_1 \varphi |x_{1i}|^{|\varphi|-1}) \\ &= (1/\alpha_i)(\dot{\hat{E}}_i^d - \hat{E}_i) + (1/\alpha_i)(\hat{E}_i + \lambda) \text{sgn}(s_i) \\ &\quad + \frac{p}{\alpha_i \sigma_2 l} x_{2i}^{[2-l/p]} (1 + \sigma_1 \varphi |x_{1i}|^{|\varphi|-1}) \end{aligned} \quad (20)$$

with $i = 1, 2, \dots, 5$.

4.2.2. Stability analysis

Define $\tilde{E}_i = \hat{E}_i - E_i$ and for stability analysis, the Lyapunov function is defined as

$$V_i = (1/2)s_i^2 + (1/2)\tilde{E}_i^2 \quad (21)$$

The derivative of V_i is

$$\begin{aligned} \dot{V}_i &= s_i \dot{s}_i + (\hat{E}_i - E_i) \dot{\hat{E}}_i \\ &= s_i \left[x_{2i} + \sigma_1 \varphi |x_{1i}|^{p-1} + \sigma_2 (l/p) \varphi |x_{2i}|^{l/p-1} (-K_p x_{2i}) \right. \\ &\quad \left. - K_{li} x_{1i} + \alpha \tau_{smi} + e_{esti} \right] \\ &+ (\hat{E}_i - E_i) \dot{\hat{E}}_i \\ &= s_i (\sigma_2 (l/p) \varphi |x_{2i}|^{l/p-1} (e_{esti} - (\hat{E}_i + \lambda) \text{sgn}(s_i))) \\ &\quad + (\hat{E}_i - E_i) s_i \sigma_2 (l/p) \varphi |x_{2i}|^{l/p-1} \text{sgn}(s_i) \\ &= s_i (\sigma_2 (l/p) \varphi |x_{2i}|^{l/p-1} (e_{esti} - (E_i + \lambda) \text{sgn}(s_i))) \\ &\leq -\sigma_2 (l/p) \varphi |x_{2i}|^{l/p-1} \lambda |s_i| \end{aligned} \quad (22)$$

Consequently, two possible cases may occur: $|x_{2i}|^{l/p-1} > 0$, $x_{2i} \neq 0$ and $|x_{2i}|^{l/p-1} = 0$, $x_{2i} = 0$. Meanwhile, considering $s_i = x_{1i} + \sigma_1 x_{1i}^{[\varphi]} + \sigma_2 x_{2i}^{[l/p]}$ when $s_i \neq 0$, two different cases are able to occur: 1) $x_{2i} \neq 0$ and 2) $x_{2i} = 0$ but $x_{1i} \neq 0$. When $s_i \neq 0$ and $x_{2i} \neq 0$, $\dot{V}_i < 0$, therefore, the system is stable according to the Lyapunov criterion when $x_{2i} \neq 0$; the system will move fast to the sliding mode surface $s_i = 0$ within finite time.

For the case $s_i \neq 0$ and $x_{2i} = 0$ but $x_{1i} \neq 0$, substituting τ_{smi} into state Eq. (12) fields

$$\dot{x}_{2i} = -(\hat{E}_i + \lambda) \text{sgn}(s_i) - \frac{p}{\sigma_2 l} x_{2i}^{[2-l/p]} (1 + \sigma_1 \varphi |x_{1i}|^{p-1}) + e_{esti} \quad (23)$$

From $x_{2i} = 0$, Eq. (23) becomes

$$\dot{x}_{2i} = -(\hat{E}_i + \lambda) \text{sgn}(s_i) + e_{esti} \quad (24)$$

Considering the equation above the system will absolutely not always keep staying on the point ($x_{2i} = 0$, $x_{1i} \neq 0$) which is thus not a terminal attractor [14]. Then the situation will return to the ones above. Therefore, it is concluded that the system will converge to $s_i = 0$ from anywhere in finite time. In addition, it is also noted that the control value does not contain any negative fractional power since $1 < l/p < 2$ and $\varphi > l/p$; thus it is singularity-free. It can be concluded that from any initial states, the closed-loop system may converge quickly to the origin along MFANFTSMC in finite time without any singularity and the chattering reduction can be realized.

Besides, the second part $(1/2)\tilde{E}_i^2$ in Lyapunov function V_i denotes the error cost of adaptive law. From Eq. (22) and the analysis above, the adaptive law eliminates the influence of E_i with the design of \hat{E}_i instead of its convergence. Therefore, the estimation of TDE error does not need converge to zero and the system error dynamics will be still Lyapunov stable.

5. Co-simulation results

Co-simulation experiments are conducted by MATLAB/SimMechanics. The time delay interval for TDE is chosen to be the same as simulation step size, i.e., the sample time.

5.1. Gait cycle definition

A concise description of gait definition is given here and the readers can get detailed illustration in our previous research [28,35]. The adjustable trajectory of left foot is given as Fig. 6.

The whole rehabilitation process can be divided into 3 parts: slow mode (0–4s), transient process (4 and 5s), fast mode (5–8s). Denoted by $q_r(t)$, the previous planned trajectory [28] is used as a basic element and the entire gait cycle is formulated as

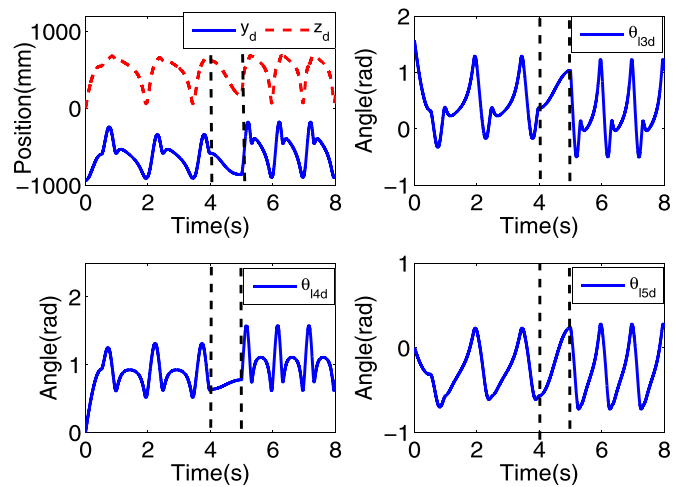


Fig. 6. The gait cycle of left leg.

$$q_d(t) = \begin{cases} q_r(t), & 0 \leq t \leq 4 \\ q_r(4) + \text{trns}(1, t-4)(1.2q_r(5) - q_r(4)), & 4 < t \leq 5 \\ 1.2q_r(5 + 1.5(t-5)), & 5 < t \leq 8 \end{cases} \quad (25)$$

where

$$\text{trns}(T_0, t) = \begin{cases} (1/2)(1 + \sin(\pi(t/T_0 - 1/2))), & t \leq T_0 \\ 1, & t > T_0 \end{cases} \quad (26)$$

is the transient function for walking mode switching. The angles of joint 1,2 are respectively set to be constant $\pi/2$ and 0 during straight walking. The walking speed of the slow mode is about 1 m/s. After transient phase (4 and 5s) which represents operator intention's impact and is marked between dotted lines, the speed of fast mode is up to about 1.5 m/s. Then, according to the inverse kinematics represented by Eq. (1), the corresponding trajectory for each joint angle can be obtained and shown as other subgraphs in Fig. 6.

5.2. Gait tracking results in joint space

For each actuator, an independent controller needs to be designed. To compare the performance of controllers, the parameters in MFC [25] and our proposed MFANFTSMC are chosen to be the same. The parameters in the co-simulation are listed as Table 3.

Fig. 7 gives the tracking errors and control torques of left leg by applying MFC and MFANFTSMC respectively. It can be observed from the figures above that the MFC achieves efficient control for the lower limb exoskeleton system during the gait tracking task and the exoskeleton can realize stable tracking. Besides, benefiting from the combination with ANFTSMC, the novel MFANFTSMC absolutely reduces the tracking errors. The control torques are limited in reasonable range and can be offered by suitable actuators.

Besides, Fig. 8 shows the tracking errors of left leg with different

Table 3
Co-simulation parameters.

Joint	1	2	3	4	5
Λ	1	1	1	1	10
K_p	20	20	15	10	50
K_I	1	1	10	15	50
p	5	5	5	5	5
l	3	3	3	3	3
φ	1.8	1.8	1.8	1.8	1.8
σ_1	10	10	20	40	80
σ_2	15	10	40	20	50
λ	1	1	1	1	1

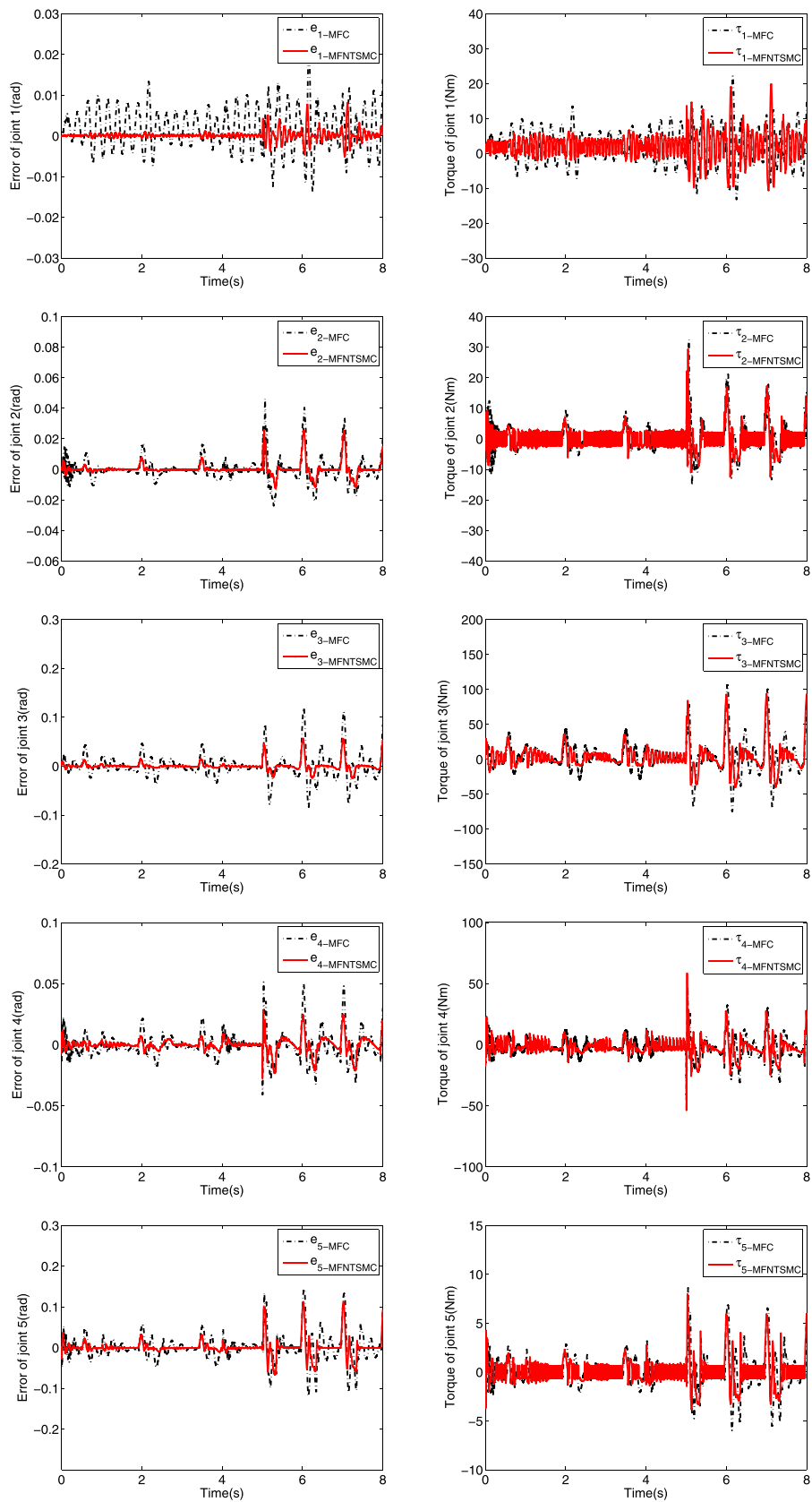


Fig. 7. Tracking errors (left column) and control torques (right column) from joint 1 to joint 5 in order.

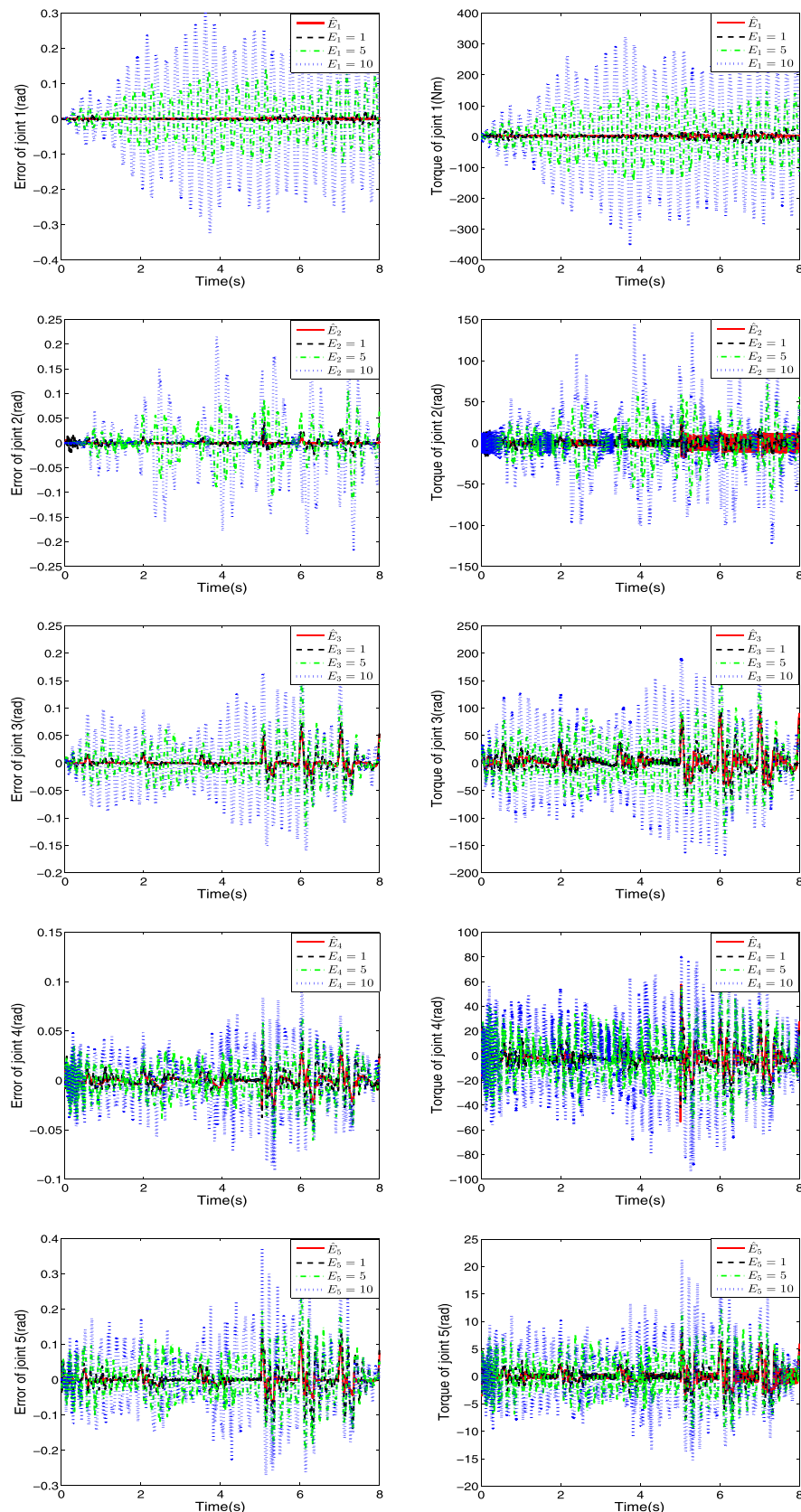


Fig. 8. Tracking errors (left column) and control torques (right column) from joint 1 to joint 5 with different switching gains in order.

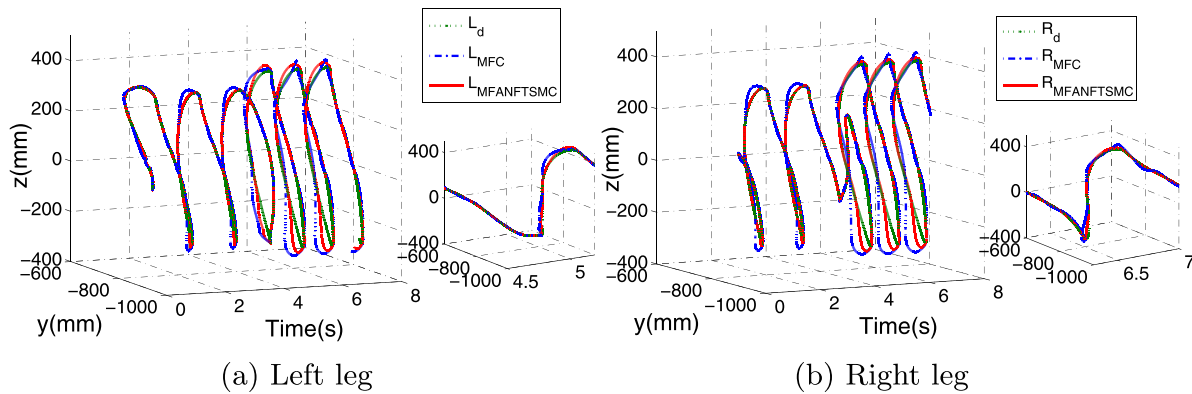


Fig. 9. Simulation results in terminal space.

switching gains to illustrate the advantages of the adaptive method. As demonstrated in Fig. 8, without adaptive approximation, the switching gain (error boundness) is determined by trials and may cause serious chattering. With adaptive approximation method, the chattering gets reduced and tracking error is smaller as well. Meanwhile, constant switching gains may increase the actuation torques or even lead to unreachable torques.

The comparative results are similar in right leg and the corresponding figures will not be listed any more.

5.3. Gait tracking results in terminal space

According to the kinematics and tracking results in joint space, the comparison results in terminal space (ankle position) are given in Fig. 9.

As the Fig. 9 illustrates, compared to the MFC, the proposed MFANFTSMC improves the tracking precision in terminal space, especially for y -axis and z -axis. As the tracking errors in x -axis are all limited in 10^{-14} (mm) magnitude, they are not shown here. Considering the maximum tracking error, the MFANFTSMC can reduce the errors by more than 50% in left foot and about 70%–80% in right foot. While the training mode switch occurs at the 4rd second, the trajectories transfer from slow mode to fast mode during the transient period (4s and 5s). Compared to MFC, the proposed MFANFTSMC shows better robustness to the tremble and can still realize more precious tracking. Observed from the zoomed figures, MFANFTSMC also shows better convergence during the transient period.

6. Conclusion

This research proposes a model independent MFANFTSMC strategy for the developed 12 DOF multi-functional lower limb exoskeleton with the virtual prototype realization in SolidWorks. Inverse kinematic solution is obtained based on the D-H theory. With the ultra-local model principle, our proposed controller combines TDE technique with adaptive SMC. To improve the tracking precision and acquire better robustness to the estimation error, NFTSMC with adaptive switching gain is combined to TDE-iPI structure, forming a novel control structure. The adaptive law is designed for the approximation of the upper bound of the uncertain part, so as to reduce the chattering causing by the large switching gain. Co-simulation results illustrate the improvement in tracking precision and robustness compared to existing MFC. The comparative results between adaptive and constant switching gains demonstrate the advantages of adaptive method in chattering reduction.

Acknowledgment

This work was partially supported by International Science & Technology Cooperation Program of China (2015DFA01710), by the

Natural Science Foundation of China (61773212, 61304077), by the Natural Science Foundation of Jiangsu Province (BK20170094) and by the 11th Jiangsu Province Six talent peaks of high level talents (2014_ZBZZ_005).

References

- [1] Bernhardt M, Frey M, Colombo G, Riener R. Hybrid force-position control yields cooperative behaviour of the rehabilitation robot lokomat. Proceedings of the IEEE 9th international conference on rehabilitation robotics. Chicago, IL, USA; 2005. p. 536–9. <http://dx.doi.org/10.1109/ICORR.2005.1501159>.
- [2] Banala SK, Agrawal SK, Kim SH, Scholz JP. Novel gait adaptation and neuromotor training results using an active leg exoskeleton. IEEE/ASME Trans Mechatron 2010;15(2):216–25. <http://dx.doi.org/10.1109/TMECH.2010.2041245>.
- [3] Pransky J. The pransky interview: Russ Angold, co-founder and president of ekso™ labs. Ind Robot Int J 2014;41(4):329–34. <http://dx.doi.org/10.1108/IR-05-2014-0334>.
- [4] Zeiling G, Weingarden H, Zwecker M, Dudkiewicz I, Bloch A, Esquenazi A. Safety and tolerance of the rewalk exoskeleton suit for ambulation by people with complete spinal cord injury a pilot study. J Spin Cord Med 2012;35(2):96–101. <http://dx.doi.org/10.1179/2045772312Y.0000000003>.
- [5] Chen B, Ma H, Qin LY, Guan X, Chan KM, Law SW, et al. Design of a lower extremity exoskeleton for motion assistance in paralyzed individuals. Proceedings of the IEEE international conference on robotics and biomimetics, ROBIO. 2015. p. 144–9. <http://dx.doi.org/10.1109/ROBIO.2015.7418758>.
- [6] Farris RJ, Quintero HA, Murray SA, Ha KH, Hartigan C, Goldfarb M. A preliminary assessment of legged mobility provided by a lower limb exoskeleton for persons with paraplegia. IEEE Trans Neural Syst Rehabilit Eng 2014;22(3):482–90. <http://dx.doi.org/10.1109/TNSRE.2013.2268320>.
- [7] Zoss AB, Kazerrooni H, Chu A. Biomechanical design of the Berkeley lower extremity exoskeleton (bleex). IEEE/ASME Trans Mechatron 2006;11(2):128–38. <http://dx.doi.org/10.1109/TMECH.2006.871087>.
- [8] Sankai Y. Hal: hybrid assistive limb based on cybernics. Robot Res Int Symp 2010;66:25–34. http://dx.doi.org/10.1007/978-3-642-14743-2_3.
- [9] Kim W, Lee H, Kim D, Han J, Han C. Mechanical design of the Hanyang exoskeleton assistive robot(hexar). Proceedings of the 14th international conference on control, automation and systems, ICCAS. 2014. p. 479–84. <http://dx.doi.org/10.1109/ICCAS.2014.6988049>.
- [10] Young AJ, Ferris DP. State of the art and future directions for lower limb robotic exoskeletons. IEEE Trans Neural Syst Rehabilit Eng 2017;25(2):171–82. <http://dx.doi.org/10.1109/TNSRE.2016.2521160>.
- [11] Le TD, Kang HJ, Suh YS, Ro YS. An online self-gain tuning method using neural networks for nonlinear pd computed torque controller of a 2-dof parallel manipulator. Neurocomputing 2013;116:53–61. <http://dx.doi.org/10.1016/j.neucom.2012.01.047>.
- [12] Song Z, Yi J, Zhao D, Li X. A computed torque controller for uncertain robotic manipulator systems: fuzzy approach. Fuzzy Sets Syst 2005;154:208–26. <http://dx.doi.org/10.1016/j.fss.2005.03.007>.
- [13] Man ZH, Paplinski AP, Wu HR. A robust mimo terminal sliding mode control scheme for rigid robotic manipulators. IEEE Trans Autom Control 1994;39(12):2464–9. <http://dx.doi.org/10.1109/9.362847>.
- [14] Feng Y, Yu XH, Man ZH. Non-singular terminal sliding mode control of rigid manipulators. Automatica 2002;38(12):2159–67. [http://dx.doi.org/10.1016/S0005-1098\(02\)00147-4](http://dx.doi.org/10.1016/S0005-1098(02)00147-4).
- [15] Van M, Ge SS, Ren H. Finite time fault tolerant control for robot manipulators using time delay estimation and continuous nonsingular fast terminal sliding mode control. IEEE Trans Cybern 2017;47(7):1681–93. <http://dx.doi.org/10.1109/TCYB.2016.2555307>.
- [16] Baek J, Jin ML, Han S. A new adaptive sliding-mode control scheme for application to robot manipulators. IEEE Trans Ind Electron 2017;63(6). <http://dx.doi.org/10.1109/TIE.2016.2522386>. 3628–3627
- [17] Lee JY, Chang PH, Jin M. Adaptive integral sliding mode control with time-delay

- estimation for robot manipulators. *IEEE Trans Ind Electron* 2017;64(8):6796–804. <http://dx.doi.org/10.1109/TIE.2017.2698416>.
- [18] Huang YJ, Kuo TC, Chang SH. Adaptive sliding-mode control for nonlinear systems with uncertain parameters. *IEEE Trans Syst Man Cybern Part B Cybern* 2008;38(2):534–9. <http://dx.doi.org/10.1109/TSMCB.2007.910740>.
- [19] Chen S-Y, Gong S-S. Speed tracking control of pneumatic motor servo systems using observation-based adaptive dynamic sliding-mode control. *Mech Syst Signal Process* 2017;94:111–28. <http://dx.doi.org/10.1016/j.ymssp.2017.02.025>.
- [20] Han JQ. From PID to active disturbance rejection control. *IEEE Trans Ind Electron* 2009;56(3):900–6. <http://dx.doi.org/10.1109/TIE.2008.2011621>.
- [21] Wang XF, Li X, Wang JH, Fang XK, Zhu XF. Data-driven model-free adaptive sliding mode control for the multi degree-of-freedom robotic exoskeleton. *Inf Sci* 2016;327:246–57. <http://dx.doi.org/10.1016/j.ins.2015.08.025>.
- [22] Hou ZS, Wang Z. From model-based control to data-driven control: survey, classification and perspective. *Inf. Sci.* 2013;235:3–35. <http://dx.doi.org/10.1016/j.ins.2012.07.014>.
- [23] Chang PH, Lee JH, Park SH. A reduced order time-delay control for highly simplified brushless dc motor. Proceedings of the american control conference. Philadelphia, Pennsylvania; 1998. p. 3791–5. <http://dx.doi.org/10.1115/1.2802514>.
- [24] Yang Y, Ma L, Huang DQ. Development and repetitive learning control of lower limb exoskeleton driven by electrohydraulic actuators. *IEEE Trans Ind Electron* 2017;64(5):4169–78. <http://dx.doi.org/10.1109/TIE.2016.2622665>.
- [25] Fliess M, Join C. Model-free control. *Int J Control Taylor* 2013;86(12):2228–52. <http://dx.doi.org/10.1080/00207179.2013.810345>.
- [26] Precup RE, Radac MB, Roman RC, Petriu EM. Model-free sliding mode control of nonlinear systems: algorithms and experiments. *Inf Sci* 2017;381:176–92. <http://dx.doi.org/10.1016/j.ymssp.2016.11.026>.
- [27] Wang HP, Ye XF, Tian Y, Zheng G, Christov N. Model-free-based terminal SMC of quadrotor attitude and position. *IEEE Trans Aerosp Electron Syst* 2016;52(5):2519–28. <http://dx.doi.org/10.1109/TAES.2016.150303>.
- [28] Wang HP, Tian Y, Han SS, Wang XK. ZMP theory-based gait planning and model-free trajectory tracking control of lower limb carrying exoskeleton system. *Stud Inf Control* 2017;26(2):161–70. <http://dx.doi.org/10.24846/v26i2y201704>.
- [29] Popovic MB, Goswami A, Herr H. Ground reference points in legged locomotion: definitions, biological trajectories and control implications. *Int J Robot Res* 2005;24(12):1013–32. <http://dx.doi.org/10.1177/0278364905058363>.
- [30] Olney SJ, Colborne GR, Martin CS. Joint angle feedback and biomechanical gait analysis in stroke patients: a case report. *Phys Ther* 1989;69(10):863–70. <http://dx.doi.org/10.1093/pjt/69.10.863>.
- [31] Denavit J, Hartenberg RS. A kinematic notation for lower-pair mechanisms based on matrices. *Trans ASME J Appl Mech* 1955;22:215–21.
- [32] Craig JJ. Introduction to robotics: mechanics and control. 3rd edition USA: Pearson Hall; 2004.
- [33] Niku SB. Introduction to robotics : analysis, control, applications. Prentice Hall; 2001.
- [34] Wang HP, Tian Y, Ni S, Christov N. Intelligent proportional trajectory tracking controllers: using ultra-local model and time delay estimation techniques. Proceedings of the 27th chinese control and decision conference, CCDC. 2015. p. 430–5. <http://dx.doi.org/10.1109/CCDC.2015.7161731>.
- [35] Wang ZF, Peyrodié L, Cao H, Agnani O, Wang H. Slow walking model for children with multiple disabilities via an application of humanoid robot. *Mech Syst Signal Process* 2016;68:608–19. <http://dx.doi.org/10.1016/j.ymssp.2015.07.010>.